

## QUANTITATIVE EVALUATION OF POROSITY IN TURBINE BLADES MADE OF IN713C SUPERALLOY AFTER HOT ISOSTATIC PRESSING

The aim of this paper is an assessment of the influence of hot isostatic pressing treatment on porosity of cast samples – turbine blades and vane clusters made of the IN713C superalloy. Two variants of HIP treatments, differing in pressure from each other, have been used.

The quantitative evaluation of the porosity was performed using light microscopy and quantitative metallography methods.

The use of the hot isostatic pressing significantly decreased the volume fraction and size of pores in the test blades, the remaining pores after the HIP process being characterized by a round shape. The increased pressure has caused significant reductions in the area fraction and size of the pores.

*Keywords:* superalloys, turbine blades, hot isostatic pressing, porosity

### 1. Introduction

The IN713C superalloy is widely used in the aerospace industry due to its low cost and good mechanical properties. The microstructure of this alloy in the as-cast state consists of  $\gamma'$  ( $\text{Ni}_3(\text{Al}, \text{Ti})$ ) particles in a  $\gamma$  matrix, primary MC carbides and  $\gamma + \gamma'$  eutectic. The  $\gamma'$  particles are characterized by their cubic shape within dendrite cores and irregular shape in the interdendritic areas [1-4]. Typical defect in as cast superalloys is gas and shrinkage microporosity (Fig. 1).

Microporosity is a microstructural defect that invariably degrades mechanical properties of superalloys castings. Microporosity is a common problem in case of casting large elements

with complicated geometry and gradation of wall thicknesses. Hot isostatic pressing (HIP) is the effective method for reducing the porosity of such castings. Hot isostatic pressing is an innovative treatment that subjects the materials to a combination of high pressure and high temperature. The processing temperature is selected in such a way that during hot isostatic pressing the material yields or creeps in compression under the applied gas pressure. Argon is the most commonly used inert gas as the pressure transmitting medium in HIP process. HIP conducted at temperatures approximating 95% of the superalloys melting temperature, under pressure in 100÷150MPa range almost totally eliminates microporosity through a combination of plastic deformation, creep, and diffusion bonding [5-7].

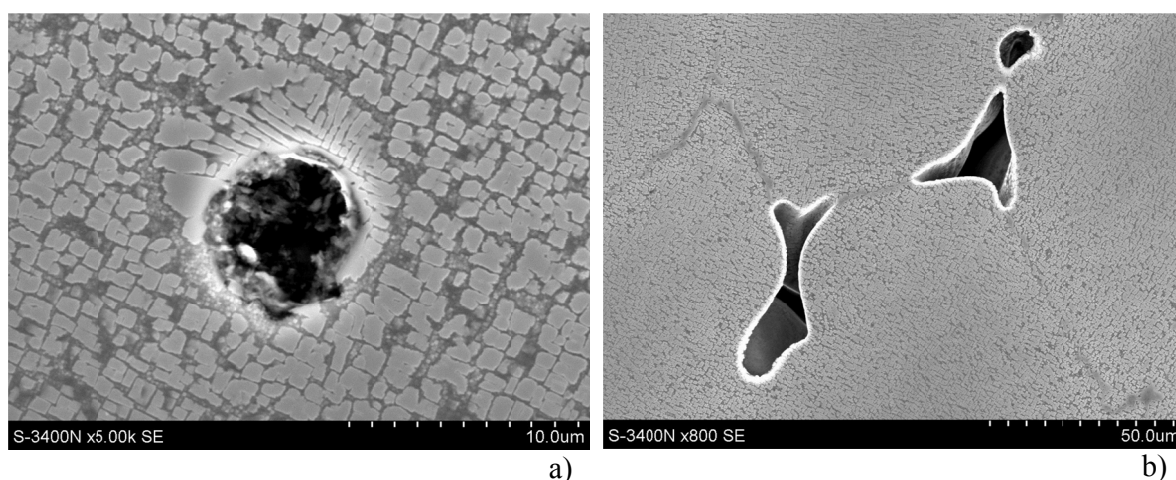


Fig. 1. Gas (a) and shrinkage porosity (b) in castings made of IN 713C superalloy

\* SILESIAAN UNIVERSITY OF TECHNOLOGY, FACULTY OF MATERIALS ENGINEERING AND METALLURGY, INSTITUTE OF MATERIALS SCIENCE, 8 KRASIŃSKIEGO STR., 40-019 KATOWICE, POLAND

<sup>#</sup> Corresponding author: stanislav.roskosz@polsl.pl

## 2. Materials and methods

The research materials were the blades and vane clusters from the aircraft engine turbine made of IN 713C superalloy, which chemical composition is presented in Table 1.

TABLE 1

The chemical composition of IN713C superalloy (in wt. %)

| Cr   | Mo  | Nb | Al | Ti  | C    | B     | Zr  | Ni      |
|------|-----|----|----|-----|------|-------|-----|---------|
| 12.5 | 4.2 | 2  | 6  | 0.8 | 0.12 | 0.012 | 0.1 | balance |

The turbine blades were used in the study in three states: as-cast (O), after 1st HIP variant – lower stress (H1) and after 2nd HIP variant – higher stress (H2). The H1 and H2 variants were characterized by the same temperature and time of the HIP. The vane clusters were used in the study in two states: as-cast (O) and after 2nd HIP variant (H2). The detailed parameters of the HIP technology are subject to export license law (confidential).

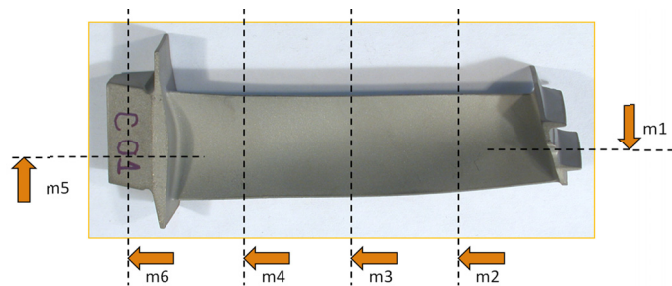


Fig. 2. IN713C superalloy blade for the porosity evaluation. Areas of metallographic measurements

The quantitative characterization of porosity has been performed using samples sectioned from the blade as shown in Fig. 2 and from the vane clusters as shown in Fig. 3. The determination of gas and shrinkage porosity was carried out on the polished samples by quantitative metallography. The complex procedure of the quantitative evaluation of gas and shrinkage porosity, described in [8], was used.

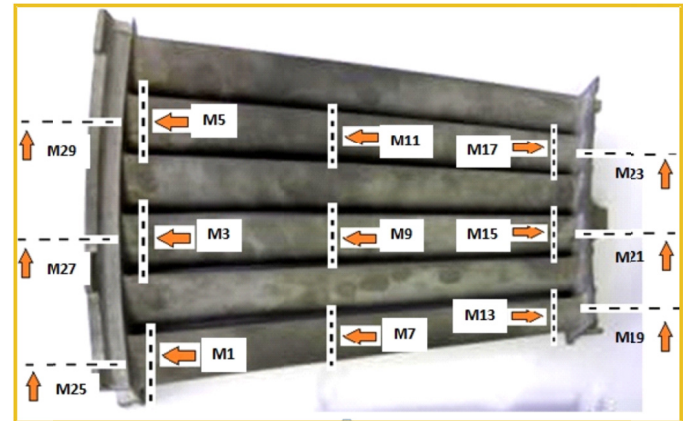


Fig. 3. IN713C superalloy vane clusters for the porosity evaluation. Areas of metallographic measurements

The samples were mechanically ground on abrasive paper (grit sizes: 320, 600, 800 and 1000), polished with diamond suspensions (grit sizes: 9  $\mu\text{m}$ , 3  $\mu\text{m}$ , 1  $\mu\text{m}$  and 0.25  $\mu\text{m}$ , respectively) and with alumina suspension (grit size: 0.05  $\mu\text{m}$ ). The samples were additionally polished using an alumina suspension (grit size: 0.05  $\mu\text{m}$ ) for 5 h with vibrations. Images of the pores were obtained using light microscope Olympus GX71 and bright field technique at 200 $\times$  magnification. The measurements were performed with Metllo15 software equipped with z macroprocedure “Porosity” for automatic detection of pores [9].

## 3. Results

The results of quantitative evaluation of pores in as cast state and after the hot isostatic pressing for turbine blades are presented in Table 2 and for the vane clusters in Table 3.

Diversification of area fraction of the pores ( $A_A$ ) [%] (mean value for each section) in as-cast state and after the HIP in blades are presented in Fig. 4 and in the vane clusters in Fig. 5. Diversification of area fraction of pores ( $A_A$ )<sub>max</sub> [%] (value for the worst field) in as cast state and after the HIP in the blades are presented in Fig. 6 and in the vane clusters in Fig. 7.

TABLE 2

The results of quantitative evaluation of porosity – the values for whole turbine blades in as-cast state (O), after I variant of HIP (H1) and after II variant of HIP (H2)

| Parameters of pores   | Symbol       | Unit             | O     | H1    | H2    |
|---|--------------|------------------|-------|-------|-------|
| <b>Amount of pores</b>  |              |                  |       |       |       |
| Area fraction – an average value for the microsection                     | $A_A$        | %                | 0.138 | 0.018 | 0.012 |
| Area fraction – a value in the worst field                                | $A_{A(max)}$ | %                | 1.310 | 0.368 | 0.062 |
| Number of pores per $\text{mm}^2$ – an average value for the microsection | $N_A$        | $\text{mm}^{-2}$ | 45.9  | 13.8  | 8.9   |
| <b>Size of the pores</b>  |              |                  |       |       |       |
| Mean plane section area   | $A$          | $\mu\text{m}^2$  | 31.7  | 18.6  | 9.9   |
| Plane section area – max value  | $A_{max}$    | $\mu\text{m}^2$  | 2480  | 942   | 126   |
| <b>Shape of the pores</b>   |              |                  |       |       |       |
| Dimensionless shape factor  | $\zeta$      | —                | 0.93  | 0.95  | 0.98  |
| <b>Heterogeneity distribution of the pores</b>                            |              |                  |       |       |       |
| Coefficient of variation of area fraction of pores                        | $v(A_A)$     | %                | 100   | 145   | 97    |

The results of quantitative evaluation of porosity – the values for whole vane clusters in as-cast state (O), after II variant of HIP (H2)

| Parameters of pores                                   | Symbol       | Unit            | O     | H2    |
|---|--------------|-----------------|-------|-------|
| <b>Amount of pores</b>                                |              |                 |       |       |
| Area fraction – an average value for the microsection | $A_A$        | %               | 0.100 | 0.010 |
| Area fraction – a value in the worst field            | $A_{A(max)}$ | %               | 2.100 | 0.117 |
| <b>Size of the pores</b>                              |              |                 |       |       |
| Mean plane section area                               | $A$          | $\mu\text{m}^2$ | 11.4  | 6.6   |
| Plane section area – max value                        | $A_{max}$    | $\mu\text{m}^2$ | 5849  | 205   |
| <b>Shape of the pores</b>                             |              |                 |       |       |
| Dimensionless shape factor                            | $\zeta$      | —               | 0.94  | 0.96  |
| <b>Heterogeneity distribution of the pores</b>        |              |                 |       |       |
| Coefficient of variation of area fraction of pores    | $v(A_A)$     | %               | 86    | 93    |

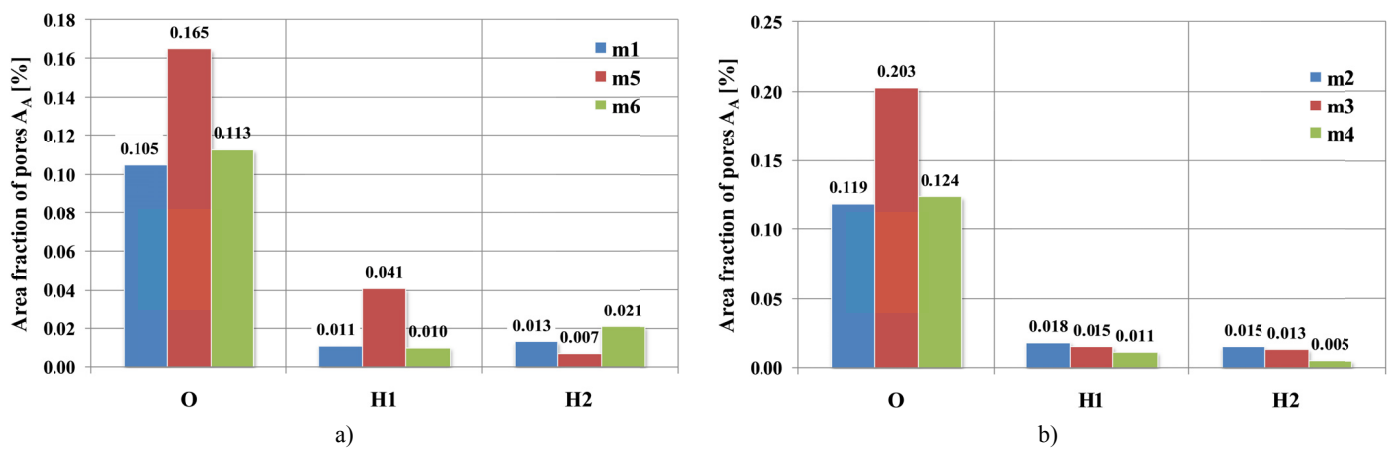


Fig. 4. Area fraction of pores  $A_A$  [%] – an average for microsections: a) root of blade, b) airfoil of blade

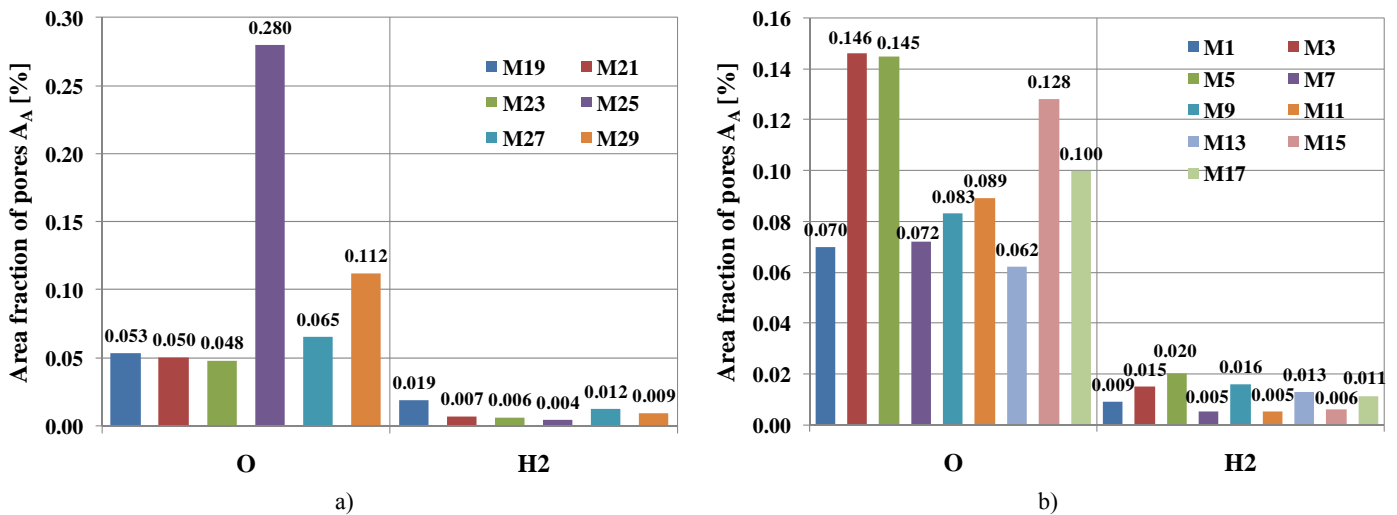


Fig. 5. Area fraction of pores  $A_A$  [%] – an average for microsections: a) root of vane cluster, b) airfoil of vane cluster

#### 4. Discussion

Comparison of the morphological parameters of the pores in the blades in as-cast state and after the HIP process has shown that the HIP caused the significant decrease of:

1. Area fraction of the pores (mean value in the whole sections) – from 0.138% in as-cast state to 0.018% after the

I variant of HIP and to 0.012% after the II variant of HIP, as well area fraction of the pores for the worst field: 1.310%, 0.368% and 0.062% respectively.

2. Number of pores per  $\mu\text{m}^2$  from 45.9  $\mu\text{m}^{-2}$  in as-cast state to do 13.8  $\mu\text{m}^{-2}$  after the I variant of HIP and to 8.9  $\mu\text{m}^{-2}$  after the II variant of HIP.

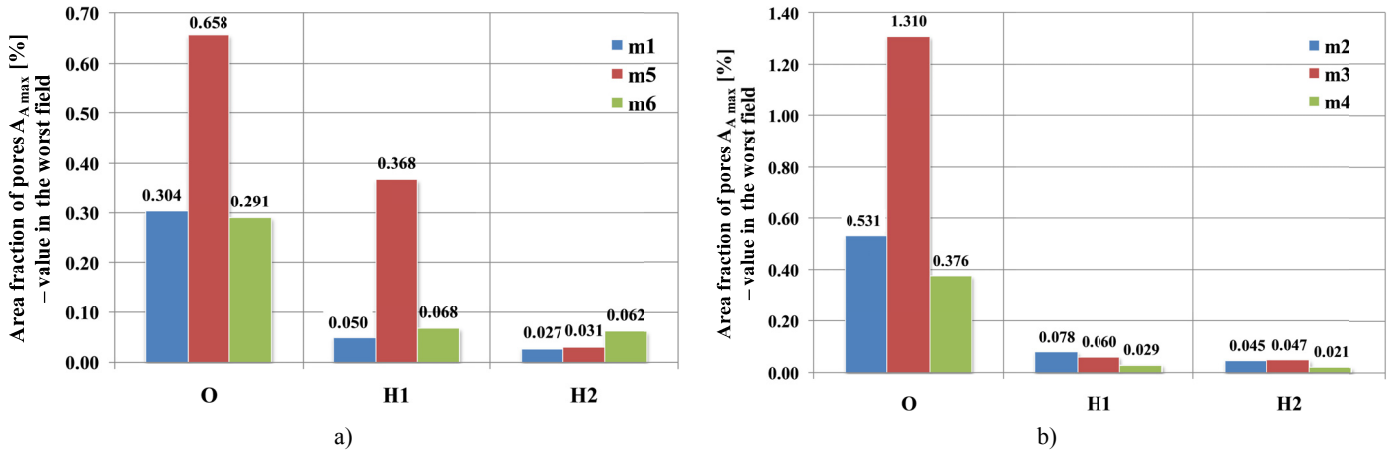


Fig. 6. Area fraction of pores  $A_{A_{max}}$  [%] – value in the worst field: a) root of blade, b) airfoil of blade

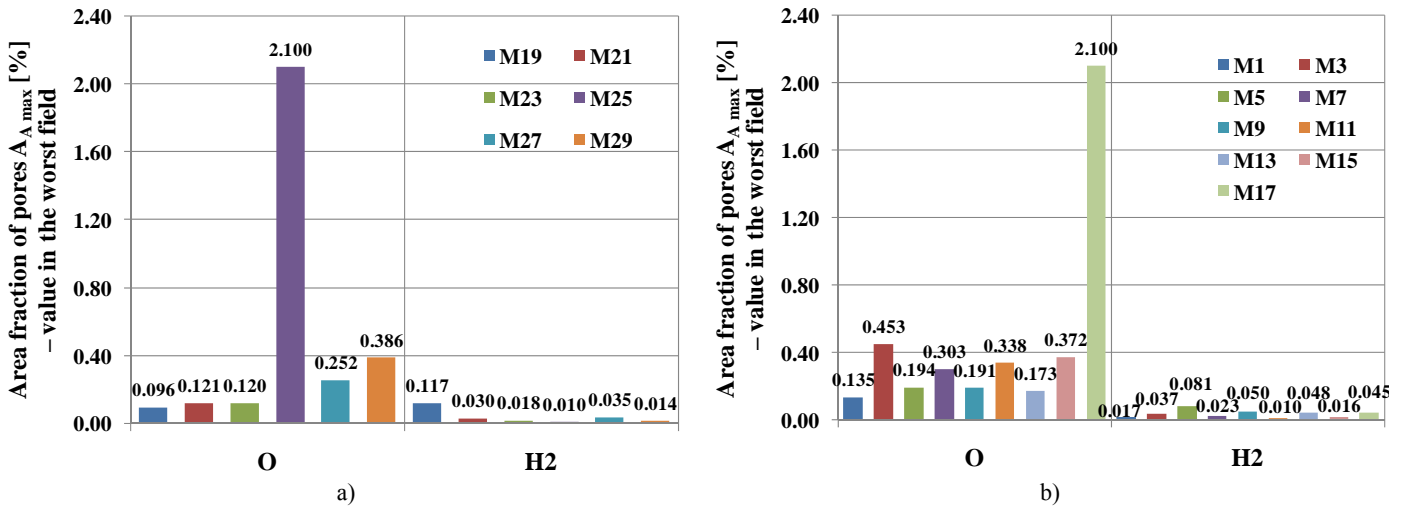


Fig. 7. Area fraction of pores  $A_{A_{max}}$  [%] – value in the worst field: a) root of vane cluster, b) airfoil of vane cluster

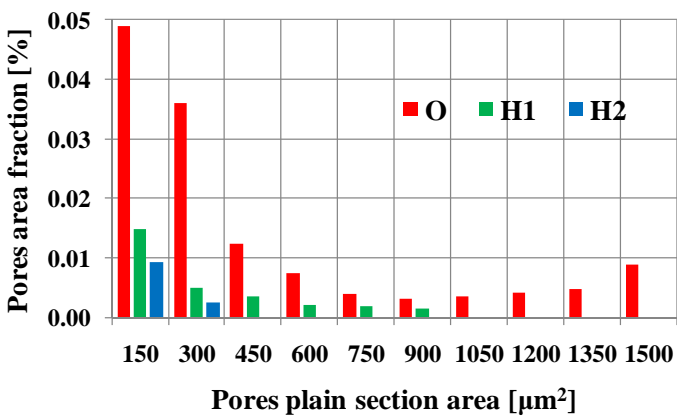


Fig. 8. Pores area fraction as function of pores plain section area

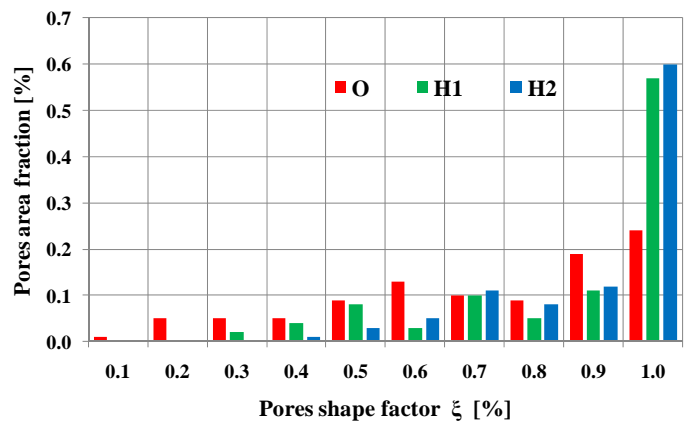


Fig. 9. Pores area fraction as function of pores shape factor

3. Pores average size (mean plane section area  $A$ ): from  $31.7 \mu\text{m}^2$  in as-cast state to do  $18.6 \mu\text{m}^2$  after the I variant of HIP and to  $9.9 \mu\text{m}^2$  after the II variant of HIP.
4. Pores maximum size (maximum plane section area  $A_{max}$ ): from  $2480 \mu\text{m}^2$  in as-cast state to  $942 \mu\text{m}^2$  after the I variant of HIP and to  $126 \mu\text{m}^2$  after the II variant of HIP.

- Comparison of the morphological parameters of the pores in the vane clusters in as-cast state and after the HIP shows, that this technology causes significant decrease of:
1. Area fraction of pores (mean value in the whole sections) – from 0.100% in as-cast state to 0.010% after the HIP and as well as in the worst field: 2.100% and 0.117% respectively.

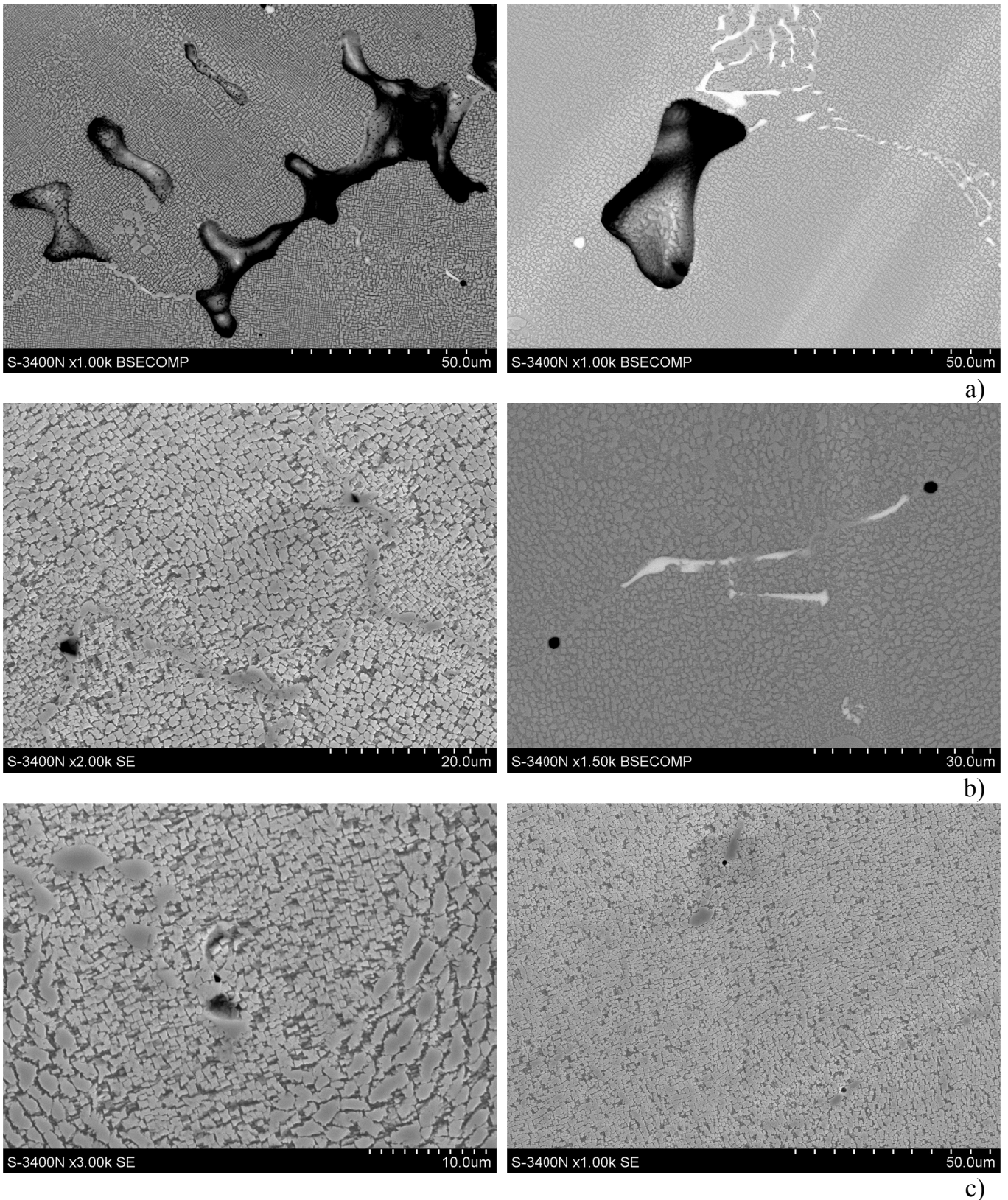


Fig. 10. Porosity in castings made of IN 713C superalloy in as-cast state (a), after I variant of HIP (b), after II variant of HIP (c)

2. Pores average size (mean plane section area  $A$ ): from  $11.4 \mu\text{m}^2$  in as-cast state to do  $6.6 \mu\text{m}^2$  after the HIP.
3. Pores maximum size (maximum plane section area  $A_{\text{max}}$ ): from  $5849 \mu\text{m}^2$  (unacceptable value in M25), to acceptable value after the HIP treatment –  $205 \mu\text{m}^2$ .

Additionally, the HIP caused the shape coefficient of pores in blades and vane clusters to monotonically increase to values close to 1, indicating that shape of the pores was more similar to that of spheres.

### 5. Conclusion

The obtained results have confirmed that the HIP process is the effective method for the elimination of microporosity of turbine blades and vane clusters made of IN 713 superalloy. The high pressures employed in HIP process have caused much larger reductions of the area fraction of the pores (worst value and average value) and size of pores. Moreover, the HIP process has caused the increase of pores shape factor indicating that shape of the pores became to be more spheroidal.

### Acknowledgements

A financial support by the Polish National Centre for Research and Development involved in the carrying-out of Project No. INNOLOT/I/8/NCBR/2013 entitled "Innovative investment casting technologies – INNOCAST" is gratefully acknowledged.

### REFERENCES

- [1] R.C. Reed, *The Superalloys: fundamentals and applications*, 2006 Cambridge University Press, Cambridge.
- [2] T.M. Pollock, S. Tin, *Nickel-based superalloys for advanced turbine engines: chemistry, microstructure and properties*, *J. Propul. Power* **22**, 361-374 (2006).
- [3] M.J. Donachie, S.J. Donachie, *Superalloys: a technical guide*, (2nd ed.)2002 ASM International.
- [4] Y. Kuang-O, et. al., *Modelling for casting and solidification processing*, 2002 Marcel Dekker Inc., New York, Basel.
- [5] L. Kunz, P. Lukáš, R. Konečná, S. Fintová, *Int. J. Fatigue* **41**, 47-51 (2012).
- [6] S.H. Chang, *J. Alloys and Compounds* **486**, 716-721 (2009).
- [7] Y. Zhou, S. Rao, Z. Zhang, Z. Zhao, *Mat. And Desing* **49**, 25-27 (2013).
- [8] S. Roskosz, M. Staszewski, J. Cwajna, *Mater. Charact.* **56**, 405-413 (2006).
- [9] S. Roskosz, *Prakt. Metallogr. PR M* **8**, 527-547 (2013).